This is an open access article published under an ACS AuthorChoice License, which permits copying and redistribution of the article or any adaptations for non-commercial purposes.

ACS Sustainable Chemistry & Engineering

Research Article

Cite This: ACS Sustainable Chem. Eng. 2019, 7, 2739−2750

pubs.acs.org/journal/ascecg

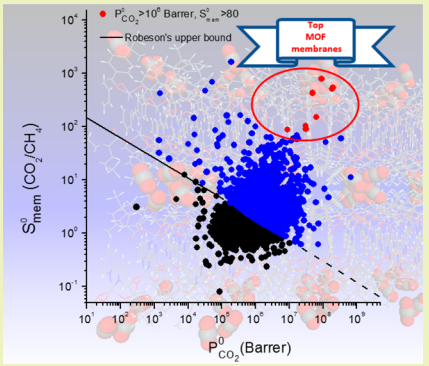
Molecular Simulations of MOF Membranes and Performance Predictions of MOF/Polymer Mixed Matrix Membranes for CO_2/CH_4 Separations

Cigdem Altintas and Seda Keskin*

Department of Chemical and Biological Engineering, Koc University, Rumelifeneri Yolu, Sariyer, 34450 Istanbul, Turkey

Supporting Information

ABSTRACT: Efficient separation of CO_2 from CO_2/CH_4 mixtures using membranes has economic, environmental and industrial importance. Membrane technologies are currently dominated by polymers due to their processing abilities and low manufacturing costs. However, polymeric membranes suffer from either low gas permeabilities or low selectivities. Metal organic frameworks (MOFs) are suggested as potential membrane candidates that offer both high selectivity and permeability for CO_2/CH_4 separation. Experimental testing of every single synthesized MOF material as membranes is not practical due to the availability of thousands of different MOF materials. A multilevel, high-throughput computational screening methodology was used to examine the MOF database for membrane-based CO_2/CH_4 separation. MOF membranes offering the best combination of CO_2 permeability (>10^6 Barrer) and CO_2/CH_4 selectivity (>80) were identified by combining grand canonical Monte Carlo and molecular dynamics simulations. Results revealed that the best MOF membranes are located above the Robeson's upper bound indicating that they outperform polymeric membranes for CO_2/CH_4 separation. The impact of framework flexibility on the membrane properties of the selected top MOFs was studied by comparing the results of rigid and flexible molecular simulations. Relations between structures and performances of MOFs were also investigated to provide atomic-level insights into the design of novel MOFs which will be useful for CO_2/CH_4 separation processes. We also predicted permeabilities and selectivities of the mixed matrix membranes (MMM) in which the best MOF candidates are incorporated as filler particles into polymers and found that MOF-based MMMs have significantly higher CO_2 permeabilities and moderately higher selectivities than pure polymers.



KEYWORDS: *Metal−organic framework, Membrane, CO_2 separation, Mixed matrix membrane, Molecular simulation*

INTRODUCTION

There is a rapidly increasing demand for the development of efficient CO_2 separation technologies due to the climate change problems. Separation of CO_2 from natural gas is a global challenge with energetic and environmental importance. CO_2 does not only reduce the energy content of the natural gas, which is mainly composed of CH_4, but also causes pipeline corrosion. Membrane-based separation of CO_2 from CH_4 has emerged as an alternative to the current energy-intensive technologies such as cryogenic distillation and chemical absorption.[1] Membrane-based separation units are easy to operate, control and scale-up. Polymeric membranes such as polyimide and polyamide have been widely utilized for CO_2/CH_4 separation due to their relatively low manufacturing costs, good processing abilities into different configurations and existence of well-documented research studies.[2] However, polymeric membranes have a trade-off between permeability and selectivity. High permeability and high selectivity are desired to achieve efficient and economic membrane-based gas separation. A selective membrane provides high purity thus requires less complex units while a membrane with high gas permeability requires less surface area and smaller capital cost. Another challenge in using polymeric membranes for commercial CO_2/CH_4 separation is the plasticization problem in which CO_2 permeability increases with pressure while the CO_2/CH_4 selectivity decreases.[3] In order to eliminate these problems, zeolites have been considered as alternatives to polymeric membranes for membrane-based CO_2/CH_4 separation. Zeolite membranes offer significantly higher CO_2/CH_4 selectivities than the polymer membranes but their low CO_2 permeabilities, high costs and difficulties in reproducibility are the main problems.[3] A zeolite membrane, SAPO-34, was reported to exceed the Robeson's upper bound by displaying both high selectivity and high permeance for CO_2/CH_4 mixtures.[4−7] Techno-economic analysis also showed that SAPO-34 membranes can surpass the benchmark technology distillation for natural gas treatment.[8]

Received: November 9, 2018
Revised: December 12, 2018
Published: December 18, 2018

Downloaded via KOC UNIV on April 9, 2019 at 09:03:27 (UTC).
See https://pubs.acs.org/sharingguidelines for options on how to legitimately share published articles.

© 2018 American Chemical Society

DOI: 10.1021/acssuschemeng.8b05832
ACS Sustainable Chem. Eng. 2019, 7, 2739−2750

Metal organic frameworks (MOFs) have appeared as a new group of porous materials that offer huge potential as membranes.[3,9−11] MOFs are composed of metal complexes combined by organic linkers to form highly porous frameworks. One of the most important features of MOFs is their structural tunabilities that can be obtained by altering the combination of metals and linkers used during synthesis. The ability of tuning the MOF structures offers a wider variety of pore sizes and functionalities than zeolites. High surface areas, large porosities, uniform pores, reasonable mechanical and thermal stabilities make MOFs ideal candidates for membrane-based CO_2 separations. Several excellent reviews have addressed a variety of novel methods to fabricate continuous, defect-free MOF membranes for CO_2 separation.[3,10,12,13] Many thin-film MOF membranes exhibit high CO_2 permeabilities and low to moderate CO_2/CH_4 selectivities.[9] Most of these membranes were fabricated using the prototype MOFs, such as MOF-5 (IRMOF-1)[14−18] and CuBTC (HKUST-1).[19−21] Zeolitic imidazolate frameworks (ZIFs) including ZIF-8, ZIF-69, ZIF-78, ZIF-90 have been widely used to make membranes.[22−24] For example, Venna and Carreon[25] fabricated reproducible, thin ZIF-8 membrane and reported that its CO_2/CH_4 selectivity ranges from ∼6.5 to 10, comparable with SAPO-34 membranes. Caro's group tested ZIF-90 membranes for separation of equimolar CO_2/CH_4 mixture at 1 bar, 498 K and reported high CO_2 permeance, 1.26×10^{-8} mol/($m^2 \times s \times Pa$) (corresponds to 753 Barrer) and CO_2/CH_4 selectivity of 4.7, which was reported to be among the MOF membranes having high separation performance.[26] In addition to pure ZIF-8 membranes, several mixed matrix membranes (MMMs) in which ZIF-8 is used as filler particles in various types of polymers have been fabricated to improve permeability and selectivity of polymer membranes. A recent review addressed the CO_2 capture, CO_2/CH_4, CO_2/H_2, and CO_2/N_2 separations using ZIF-8-based MMMs by summarizing the fabrication techniques and special features of each membrane.[27] MOF-based MMMs are highly promising since they combine the two advantages of polymers and MOFs, easy processability and high gas permeability.

The number of MOFs is increasing rapidly and this large material space offers a great potential to be used as novel membranes for CO_2/CH_4 separation. Many MOFs might exhibit high CO_2/CH_4 separation potential but they have not been identified and tested yet. Experimental fabrication and testing of even a single MOF membrane require a long time, extensive efforts and resources. Similarly, choosing the best MOF filler to make MMMs is challenging because many MOFs and polymers are available resulting in infinite number of MOF/polymer combinations. Therefore, only a small fraction of MOFs has been experimentally examined as membranes and/or as fillers in MMMs to date and molecular simulations that screen many MOFs to identify the best materials have a vital role in directing experimental efforts.[28] Computational screening studies generally focus on adsorption-based H_2/CH_4, CO_2/N_2, and CO_2/CH_4 separations and grand canonical Monte Carlo (GCMC) simulations are used to compute gas adsorption in MOFs.[29−32] The number of studies on screening MOF membranes is very limited since assessing selectivity and permeability of a MOF membrane requires calculation of gas diffusivities in the MOFs' pores using equilibrium molecular dynamics (MD) simulations, which is computationally very demanding compared to the GCMC simulations. Watanabe and Sholl[33] used molecular simulations to compute CO_2/N_2 separation performances of 179 MOFs and reported ideal selectivities in the range of 2−26 300 and CO_2 permeabilities in the range of $2-6 \times 10^7$ Barrer. Daglar and Keskin[34] examined 3806 MOF membranes for CO_2/N_2 separations and identified the best MOF membranes having CO_2/N_2 selectivity >350 and CO_2 permeability $>10^6$ Barrer. Qiao et al.[35] used molecular simulations to screen a large number of hypothetical MOFs, which are computer-generated materials, for membrane-based separation of $CO_2/N_2/CH_4$ mixture. The top 24 hypothetical MOFs were identified and their CO_2 selectivities were reported to be in the range of 260−10 500 at 10 bar and 298 K. The same group also carried out molecular simulations for separation of ternary $CO_2/N_2/CH_4$ mixture using real MOFs at 10 bar, 298 K and reported CO_2 selectivities of MOFs in the range of 700−8100 and CO_2 permeabilities >1000 Barrer for the 7 best MOF materials.[36] Our group recently used high-throughput screening methods to examine >3500 MOF membranes for H_2/CH_4 separation[37] and H_2/CO_2 separation.[38] Results showed that many MOF membranes outperform polymer and zeolite membranes in terms of H_2 selectivity and H_2 permeability. An important point to note is that previous computational works were performed using rigid framework assumption, where the crystallographic positions of MOF atoms were fixed. Significant computational time is saved due to this assumption, however flexibility of MOFs might affect gas diffusion and eventually change the predicted performances of MOF membranes.[39,40] Therefore, the effect of flexibility on CO_2/CH_4 separation performance of at least some of the most promising MOF membranes deserves to be examined.

With these motivations, we applied a multilevel, high-throughput computational screening methodology showing increasing computational expense and complexity at each level to study the most recent MOF database reported in the literature.[41] This database has been only studied for membrane-based CO_2/N_2 separation[34] and CO_2/H_2 separation[38] but not for CO_2/CH_4 separation. In the first-level of screening, we calculated CO_2 permeabilities and CO_2/CH_4 selectivities of MOF membranes using single-component gas adsorption and diffusion data obtained from the GCMC and MD simulations performed at infinite dilution. Predicted separation performances of MOF membranes were compared with polymeric and zeolite membranes. The top 8 MOF membranes exhibiting CO_2 permeabilities $>10^6$ Barrer and CO_2/CH_4 selectivities >80 were identified. In the second-level of calculations, we carried out GCMC and MD simulations for the top MOF membranes considering equimolar CO_2/CH_4 mixtures. Impacts of adsorption and diffusion on the separation performance of the top membranes were investigated in detail. In the third level of calculations, framework flexibility was considered and its impact on the membrane properties of MOFs was studied by comparing the results of rigid and flexible MD simulations. Relations between structures and performances of MOFs were also investigated to provide atomic-level insights into the design of novel MOFs which will be useful for CO_2/CH_4 separation processes. Finally, the potential of using top MOFs as filler particles in polymer membranes was examined by computing gas permeability and selectivity of MOF/polymer MMMs for separation of CO_2/CH_4 mixture. The results presented in this study will be beneficial in guiding the selection of the best MOF membranes and MOF-based MMMs for natural gas purification process.

DOI: 10.1021/acssuschemeng.8b05832
ACS Sustainable Chem. Eng. 2019, 7, 2739−2750

MOLECULAR SIMULATIONS

The most recent MOF database[41] reported in the literature was used in this work. Solvent molecules were removed from the structures as described in the literature[41] and Zeo++ software[42] (version 0.2) was utilized to calculate pore limiting diameters (PLDs), the largest cavity diameters (LCDs), porosities and surface areas of MOFs. More details of these calculations are available in our earlier studies.[32,34] This MOF database was refined to only include materials with nonzero accessible surface areas and PLDs > 3.75 Å to let the permeation of both CO_2 (3.3 Å) and CH_4 (3.73 Å) through the membranes. We also excluded the MOFs for which molecular simulations resulted in gas diffusivities $<10^{-8}$ cm^2/s, which is the limit of MD to accurately characterize molecular diffusion. As a result, we ended up with 3794 MOFs having various structural properties.

Molecular simulations were initially performed to calculate the Henry's constants (K^0) and self-diffusivities (D^0) of CO_2 and CH_4 at infinite dilution using the RASPA simulation code.[43] The adsorbate−adsorbate interactions were switched-off and 30 gas molecules were inserted into each MOF to imitate infinite dilution. The Widom particle insertion method was used to calculate K^0 of each gas at 298 K.[44] For the Monte Carlo simulations, the number of initialization and production cycles was set to 5000 and 10 000, respectively. The mean square displacement of gas molecules was computed and its slope with respect to time obtained from the MD simulations was used to calculate D^0 of each gas component. MD simulations were performed in the NVT ensemble using the Nosé−Hoover thermostat[44] for 10^6 cycles with a time step of 1 fs. Lennard-Jones (LJ) potential was used to define intermolecular interactions between the gases and MOFs. CO_2 molecule was modeled as a three-site rigid molecule and its partial point charges were positioned at the center of each site.[45] CH_4 was modeled as a single-sphere. Potential parameters and charges of gases are given in Table S1 of Supporting Information (SI). The Universal Force Field (UFF)[46] was used to define the potential parameters of MOFs. Charge equilibration method (QEq)[47,48] existing in RASPA was employed to assign partial point charges to MOF atoms and electrostatic interactions between MOFs and CO_2 were calculated using the Ewald summation.[49] The good agreement between simulations and experiments for adsorption and diffusion properties of CO_2 and CH_4 in various MOFs was shown in our earlier studies[32,50,51] and validated the appropriateness of the selected force fields for MOFs and gas molecules. The UFF was developed a long time ago and it has the advantage of being adaptable to many chemical environments. However, it may not be suitable for certain materials such as MOFs having open metal sites. For example, Dzubak et al.[52] reported that common force fields (FFs) typically underestimate CO_2 adsorption in Mg-MOF-74 which have open metal sites and presented a novel methodology that gives accurate FFs for CO_2 adsorption in this MOF from high-level quantum chemical calculations. There have been more recently parametrized FFs which have been shown to be more appropriate for MOFs.[53,54] For example, Bristow et al.[54] developed a transferable potential form suitable to describe majority of ligand and metal combinations for MOFs. In contrast to UFF, in which general parameters were not fitted for MOFs and fixed generic charges were employed, their FF was fitted explicitly to the periodic frameworks and it was shown to accurately reproduce structural parameters of several MOFs. We used UFF in our molecular simulations for two reasons: (a) We previously showed the good agreements between simulations employing UFF and experiments for adsorption and diffusion of CO_2 and CH_4 in various MOFs, validating the appropriateness of UFF for MOFs as explained above. (b) We preferred a generic FF that is applicable to all types of MOFs in our high-throughput molecular simulations since it is not possible to perform high-level quantum chemical calculations for each MOF having open metal site in large scale material screening studies. Therefore, molecular simulations using the generic UFF may be underestimating CO_2 adsorption and CO_2 separation performances of MOFs having open metal sites.

Gas permeabilities of MOFs at infinite dilution (P_i^0) were calculated using $P_i^0 = K_i^0 \times D_i^0$. Ideal CO_2/CH_4 selectivities of MOF membranes were calculated as the ratio of gas permeabilities, $S_{mem}^0 = P_{CO_2}^0/P_{CH_4}^0$. Top 8 MOFs having high membrane selectivities, $S_{mem,\ CO_2/CH_4}^0 > 80$ and high CO_2 permeabilities, $P_{CO_2}^0 > 10^6$ Barrer were identified at the end of first-level of calculations. In the second-level of calculations, we computed adsorption of binary CO_2/CH_4:50/50 mixtures in top 8 MOFs. Binary mixture simulations were performed at two different pressures, 1 and 10 bar, at 298 K. In contrast to the first-level of calculations, both gas−gas and gas−MOF interactions were taken into account in the mixture simulations. Intermolecular interactions were truncated at a cutoff distance of 13 Å. A total of 15 000 cycles was used, where 5000 cycles were used for initialization and 10 000 cycles were used to obtain the ensemble averages. GCMC simulations of equimolar CO_2/CH_4 mixtures performed at 1 and 10 bar, at 298 K were used to define the initial states of mixture MD simulations. After 10 000 initialization and 10 000 equilibration cycles, 10^7 cycles were used to obtain mean square displacement of gases in the NVT ensemble using a time step of 1 fs. Gas diffusivities were computed using at least two trajectories. More details about using these simulations can be found in the literature.[44,55] Mixture permeabilities through MOF membranes were computed using $P_i^{mix} = c_i^{mix} \times D_i^{mix}/f_i$ where c_i, D_i and f_i correspond to adsorbed gas loading, self-diffusivity and feed side partial pressure of the gas, respectively. Permeate side of the membrane was assumed to be vacuum.[56] Mixture selectivities were computed as the ratio of gas permeabilities using $S_{mem}^{mix} = P_{CO_2}^{mix}/P_{CH_4}^{mix}$. It is important to note that we previously validated the accuracy of this computational methodology by showing the good agreement between our predictions and experimentally measured permeances/permeabilities of single-component CO_2 and CH_4 gases through MIL-53-Al,[57] Ni-MOF-74,[34,37,38,57] IRMOF-1,[34,37,57] ZIF-69,[57] ZIF-78,[57] ZIF-90,[34,37,57] ZIF-95[34,37] membranes and even for the equimolar mixture permeability of CO_2 and CH_4 through ZIF-69 membranes.[57]

In the third-level of calculations, flexible MD simulations were performed using the Forcite module of Materials Studio 17.2[58] to study the influence of flexibility on the predicted membrane performances of MOFs. Due to the computational expense of the flexible MD simulations, only 2 of the top 8 MOFs were simulated and these MOFs were selected based on their pore sizes to represent a narrow-pored MOF (LOYMET, PLD:3.98 Å) and a large-pored MOF (KIPJUQ, PLD: 7.29 Å). Before starting the flexible MD simulations, the number of gas molecules that was computed using mixture GCMC

DOI: 10.1021/acssuschemeng.8b05832
ACS Sustainable Chem. Eng. 2019, 7, 2739−2750

simulations were loaded into the MOFs by the Fixed Loading task of the Sorption module. The force fields used in RASPA were employed in the Sorption module of Materials Studio. Both the equilibration and production steps were set to 5×10^6. van der Waals interactions were summed with atom-based interaction method with cubic spline truncation, cutoff distance of 13 Å and spline width of 1 Å were used in the Fixed Loading simulations. Partial charges for the framework atoms were assigned using QEq[48] charge method as implemented in the Materials Studio. Electrostatic interactions were summed with the Ewald summation method with an Ewald accuracy of 10^{-3} kcal/mol. Further information on performing these simulations using Materials Studio can be found in the literature.[59] The lowest energy frame obtained at the end of the fixed loading simulation was used for the flexible MD simulations which were performed in NVT ensemble with a step size of 1 fs up to a total of 10 ns by removing the fixed constraints on each coordinate of the MOF atoms. Initial velocities of gas molecules were randomly assigned. Similar to the rigid simulations, UFF and Nosé−Hoover thermostat were used in the flexible MD simulations. We validated the generic FF parameters used in flexible MD simulations of MOFs by comparing the experimental and simulated gas permeabilities in our previous work.[60] A recent work[61] also showed that results obtained with the UFF description of MOF flexibility is quantitatively comparable with the Density-Functional Tight-Binding (DFTB) predictions. To evaluate the differences between the results of rigid and flexible MD simulations, the changes in pore sizes of the MOFs were investigated. Crystal structures of MOFs were recorded at different time points during the flexible MD simulations using Materials Studio and pore sizes of materials were computed using Zeo++.

Finally, we examined the potential of MOF-based MMMs by estimating their gas permeabilities and selectivities. The top 8 MOFs were used as filler particles in 8 different types of polymers including the widely used ones such as cellulose acetate,[62] Matrimid,[63] polysulfone,[64] SPEEK-3 (sulfonated aromatic poly(ether ether ketone)),[65] Pebax (poly(ether-*b*-amide-6),[66] 6FDA-DAM (6FDA: 2,2-bis (3,4-carboxyphenyl) hexafluoropropane dianhydride and DAM: diaminomesitylene),[67] PIM-1 (polymer of intrinsic microporosity)[68] and PIM-6FDA-OH (6FDA: hexafluoroisopropylidene bisphthalic dianhydride).[69] These polymers were selected considering availability of the experimental permeability data for CO_2/CH_4 mixture. We previously studied numerous permeation models such as Maxwell, Bruggeman, Lewis-Nielson, Pal by comparing permeabilities obtained from these models with the available experimental data for CO_2 and CH_4 permeabilities of many MOF-based MMMs and concluded that Maxwell is the most appropriate model among the ones using the ideal morphology concept to estimate separation performances of MOF/polymer MMMs.[70] Therefore, we used the Maxwell model[71] to predict gas permeabilities of the MOF-based MMMs (P_{MMM}) using the following expression:

$$P_{MMM} = P_p \times \frac{n \times P_{MOF} + (1-n) \times P_p - (1-n) \times \phi \times (P_p - P_{MOF})}{n \times P_{MOF} + (1-n) \times P_p + n \times \phi \times (P_p - P_{MOF})} \quad (1)$$

where n is the geometry shape factor taken as 0.3 assuming sphere-like MOF particles,[72] ϕ is the volume fraction of the MOF particles in the polymer matrix, P_{MOF} is the gas permeability of MOF, P_p is the gas permeability of polymer collected from the literature, and P_{MMM} is the gas permeability of the MOF-based MMM. Since the Maxwell model was reported to be valid at low filler loadings,[72] we used ϕ as 0.2 in this work. If the permeability of polymer was measured at a feed pressure lower than 5 bar (Pebax and 6FDA-DAM), permeability of MOF computed at 1 bar was used for the Maxwell model, for all other polymers, permeability of MOF calculated at 10 bar was used.

RESULTS AND DISCUSSIONS

We first computed K^0 and D^0 values of CO_2 and CH_4 in 3794 MOFs as shown in Figure 1a. K^0 can be considered as the

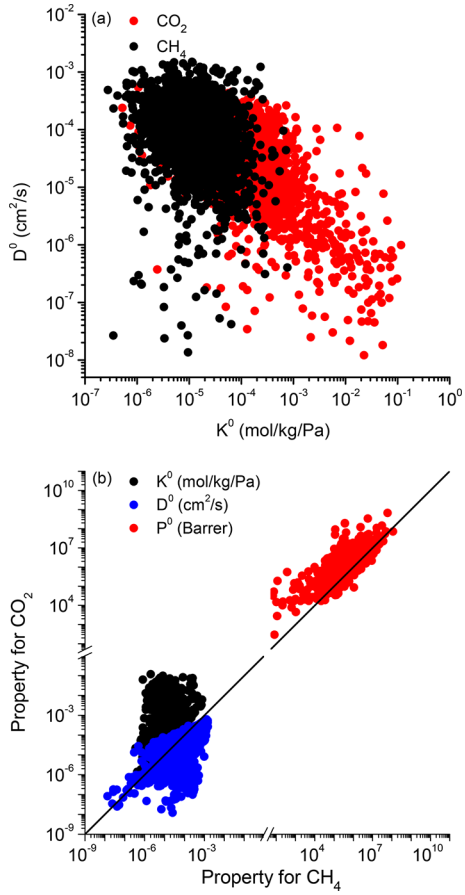


Figure 1. (a) Self-diffusivity of gases (D^0) as a function of Henry's constants (K^0) calculated at infinite dilution. (b) Comparison of K^0, D^0, and P^0 values of gases.

representative of the gas affinity of materials and as it gets higher, interaction of gas molecules with the adsorption sites of MOFs increases leading to stronger adsorption. K^0 values vary between 10^{-7} and 10^{-1} mol/kg/Pa for CO_2 and between 10^{-7} and 10^{-4} mol/kg/Pa for CH_4. Higher K^0 values of CO_2 can be explained by the existence of three interaction sites of CO_2 molecule compared to the single-sphere representation of CH_4 in addition to the quadrupolar moment of CO_2, which causes electrostatic interactions with the MOFs that are absent in the case of nonpolar CH_4 molecules. The values of D^0 vary between 10^{-8} and 10^{-4} cm^2/s for CO_2 and between 10^{-8} and 10^{-3} cm^2/s for CH_4. Since CH_4 molecules are weakly adsorbed in MOFs and lighter compared to CO_2 molecules, they are able to move faster. Strongly adsorbing gas molecules need to overcome a larger interaction energy barrier to move through the pores whereas diffusion of the weakly adsorbed gas

DOI: 10.1021/acssuschemeng.8b05832
ACS Sustainable Chem. Eng. 2019, 7, 2739−2750

molecules is easier.[73] Therefore, there is an inverse relationship between K^0 and D^0 of gases as shown in Figure 1a. This relationship is less linear for CH_4 molecules because in some MOFs, PLDs are very close to the kinetic diameter of CH_4, which leads to very slow diffusion of CH_4 even though K^0 is low. It is important to note that MOFs for which gas diffusivities were calculated to be less than 10^{-8} cm^2/s (the limit of MD simulations to accurately access gas diffusivity on the nanosecond scale) were eliminated in our work. The MOFs having high diffusion selectivities due to the presence of very slow diffusing gas molecules might be highly selective membranes, but we eliminated them to remove the uncertainties resulting from the time scale limitation of MD simulations.

The relationship between K^0 and D^0 determines gas permeabilities ($P_i^0 = K_i^0 \times D_i^0$) as shown in Figure 1b and drives the membrane-based separation performances of MOFs. K^0 always favors CO_2 molecules whereas D^0 mostly favors CH_4 molecules. As a result, gas permeabilities of MOFs are generally close to each other but mostly higher for CO_2 than CH_4 as shown in Figure 1b. Kim et al.[73] discussed that zeolite membranes should have well-balanced adsorption−diffusion properties for the effective CO_2/CH_4 separation: If the zeolites have very small $K^0_{CO_2}$ values, CO_2 permeability and selectivity is too low. If structures have very large $K^0_{CO_2}$ values, they have strong adsorption sites that significantly hinder gas diffusion. They showed that optimal zeolite membranes with the highest CO_2 permeabilities (>10^5 Barrer) have $10^{-5} < K^0_{CO_2} < 10^{-4}$ mol/kg/Pa. We showed the combined effects of K^0 and D^0 on gas permeabilities of MOF membranes in Figure S1. Analyzing MOFs exhibiting high CO_2 permeabilities (>10^6 Barrer) showed that 1787 highly permeable MOFs have $10^{-6} < K^0_{CO_2} < 10^{-1}$ mol/kg/Pa whereas 702 of them have $10^{-5} < K^0_{CO_2} < 10^{-4}$ mol/kg/Pa. This comparison shows that MOFs we examined in this work have a wider range of $K^0_{CO_2}$ values than the zeolites. The highest CO_2 permeability, 6.72×10^8 Barrer, belongs to the MOF having $K^0_{CO_2}$ of 1.85×10^{-2} mol/kg/Pa, indicating the strong affinity of MOF toward CO_2.

We examined adsorption selectivity ($S^0_{ads} = K^0_{CO_2}/K^0_{CH_4}$), diffusion selectivity ($S^0_{diff} = D^0_{CO_2}/D^0_{CH_4}$) and membrane selectivity (also known as perm-selectivity) calculated at the infinite dilution ($S^0_{mem} = P^0_{CO_2}/P^0_{CH_4} = (K^0_{CO_2} \times D^0_{CO_2})/(K^0_{CH_4} \times D^0_{CH_4})$) in Figure 2. S^0_{ads} is always higher than 1 which means all the MOFs selectively adsorb CO_2 over CH_4. While S^0_{ads} ranges from 1.2 to 7.82×10^4, S^0_{diff} tends to favor CH_4. MOFs shown in Figure 2 are color-scaled according to their S^0_{diff} values, ranging from 3.86×10^{-4} to 58. Red, green and blue points show MOFs having strong, moderate and low S^0_{diff} values for CH_4 over CO_2, respectively. Small numbers of MOFs shown with purple points (395 MOFs) have S^0_{diff} values equal to or higher than unity, indicating that diffusivity favors CO_2 over CH_4 in these materials. When both adsorption and diffusion favor the same gas molecule, CO_2, membrane selectivity becomes higher than the adsorption selectivity. In fact, those are the highly desired membrane materials for selective separation of CO_2 from CH_4. For the other 3399 MOFs, CH_4 has higher diffusivity through the MOFs' pores, therefore S^0_{diff} values are less than unity as shown with red, green and blue points in Figure 2. In this case, S^0_{mem} could not reach as high values as S^0_{ads} because diffusion selectivity favoring CH_4

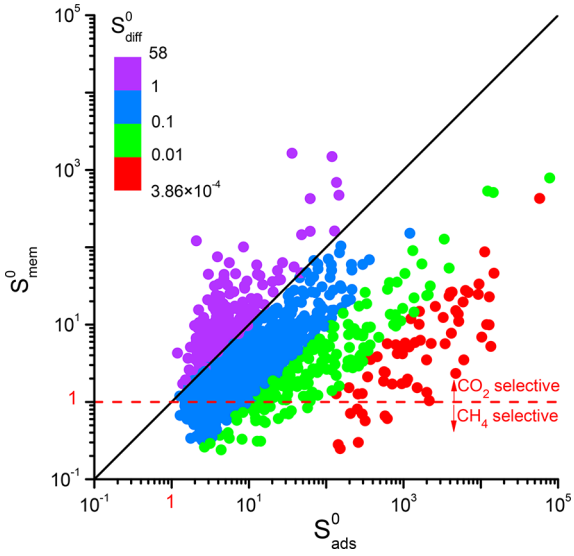


Figure 2. Adsorption, diffusion and membrane selectivities of MOFs calculated for CO_2 over CH_4 separation at infinite dilution. The diagonal line is given to guide the eye, the dashed line shows the gas preference of the membrane.

compensates adsorption selectivity favoring CO_2. 429 MOFs have S^0_{mem} lower than 1. For these MOFs, it can be concluded that CO_2 adsorption is not strong enough to dominate the fast CH_4 diffusivity. These MOFs are shown below the red dashed line in Figure 2 as CH_4 selective MOF membranes and CO_2 can be obtained in the retentate stream rather than the permeate when this type of membrane is used. We note that the maximum CH_4 selectivity of these membranes was calculated to be 12.5 indicating that they are at most moderately CH_4 selective. Eleven MOFs were predicted to have S^0_{mem} of exactly 1 which means these membranes are not useful for selective separation of CO_2 from CH_4. A large number of MOFs (3354) was computed to have S^0_{mem} larger than 1 and these CO_2 selective MOF membranes are shown above the red dashed line in Figure 2. As we discussed in Figure 1b, some MOFs have similar CO_2 and CH_4 permeabilities, therefore their CO_2 selectivities are low. For example, 1598 MOFs have S^0_{mem} between 1 and 2 indicating that they do not have a very strong preference for CO_2. These are the MOFs for which adsorption selectivity for CO_2 is almost the same with diffusion selectivity that prefers CH_4 and as a result the membrane is almost nonselective. The remaining 1756 MOFs have S^0_{mem} between 2 and 1643 and these are the potential membrane candidates.

For an efficient membrane-based gas separation process, not only the purity (selectivity) but also the amount of gas transported through the membrane (permeability) is critical because the required surface area of membrane is the dominant factor determining the cost of the separation process. Figure 3 represents the membrane selectivity (S^0_{mem}) as a function of CO_2 permeability ($P^0_{CO_2}$) together with the famous Robeson's upper bound, which is established based on the single-component CO_2 permeability and ideal CO_2/CH_4 selectivity of polymeric membranes.[74] In contrast to the well-known trade-off of polymeric membranes between the gas permeability and selectivity, permeability of MOF membranes usually increases as the selectivity increases. Predicted CO_2 permeability of MOFs varies between 10^2 and 10^8 Barrer,

DOI: 10.1021/acssuschemeng.8b05832
ACS Sustainable Chem. Eng. 2019, 7, 2739−2750

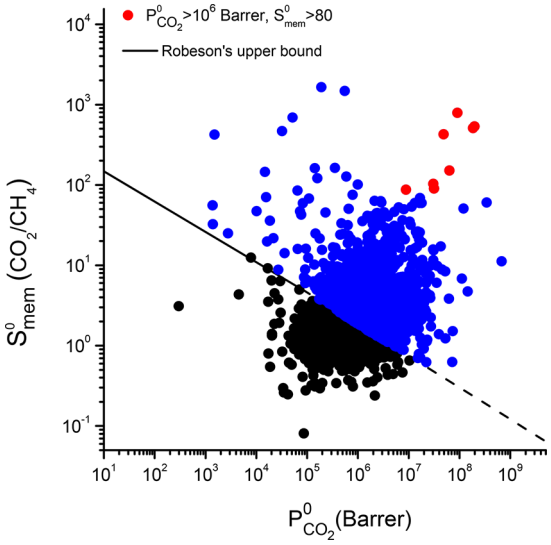


Figure 3. Selectivity and permeability of MOF membranes computed at infinite dilution. The black solid line represents the Robeson's upper bound. MOFs that can exceed the bound are shown with blue and the top 8 MOF membranes are shown with red symbols.

significantly higher than the corresponding permeabilities of polymeric membranes. Therefore, the upper bound was extended with a dashed line in Figure 3. There are 1995 MOFs that can exceed Robeson's upper bound due to their high permeabilities, or their high selectivities or both and these are shown with blue points. The most promising MOF membranes that will be further examined in the second-level of screening were selected as the materials that offer $P^0_{CO_2} > 10^6$ Barrer and $S^0_{mem} > 80$. 1483 MOFs that are over the upper bound have $P^0_{CO_2}$ higher than 10^6 Barrer while 8 of these MOFs have S^0_{mem} higher than 80. These 8 MOFs, which are shown with red in Figure 3, are identified as the top membrane materials. We would like to note that all the MOFs we considered in our work are real, synthesized MOFs, they are not hypothetical materials. However, none of the top MOFs has been tested as membranes yet.

In the second-level of screening, we computed adsorption and diffusion of equimolar CO_2/CH_4 mixtures for the top 8 MOFs and predicted mixture permeabilities and selectivities of these top MOF materials. Figure 4a compares permeability and selectivity predictions obtained at the first-level of screening (using single-component gas data at infinite dilution) and predictions obtained at the second-level (using equimolar mixture data at 1 and 10 bar). As shown in Figure 4a, both CO_2 permeabilities and CO_2/CH_4 selectivities obtained from the mixture simulations performed at practical operating pressures are lower than the ones obtained from the single-component gas simulations performed at infinite dilution. This difference can be attributed to the competitive adsorption and collaborative diffusion between gas species in the mixture. At infinite dilution, a gas molecule can prefer the most favorable adsorption site since the intermolecular interactions between the gases are turned-off. However, at mixture conditions, gas–gas interactions exist and adsorbates compete with each other for the same adsorption sites. Moreover, at infinite dilution, self-diffusivity of a gas molecule is not affected by the diffusivity of another gas molecule. On the other hand, at mixture conditions, fast diffusing gas species (CH_4) can fasten

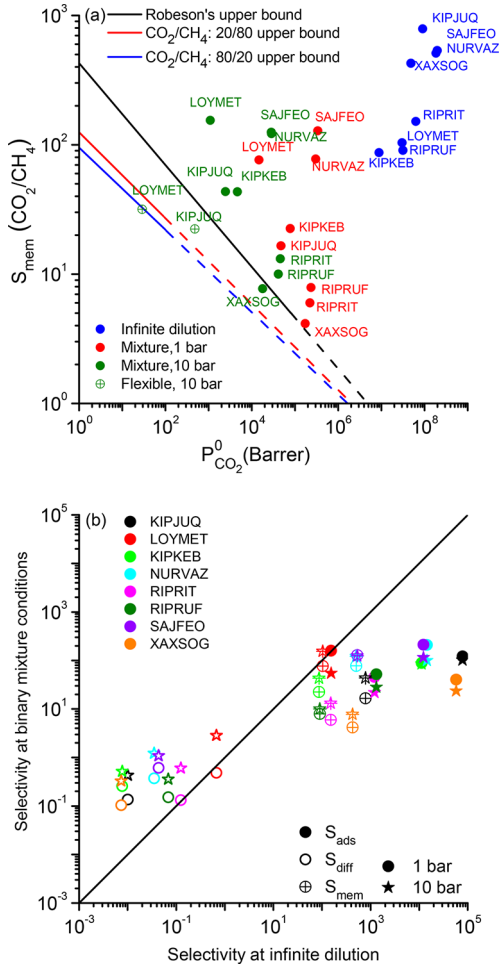


Figure 4. (a) Separation performance of the top 8 MOF membranes computed at infinite dilution (blue), 1 bar (red), and 10 bar (green). Results of flexible simulations for the two MOFs are also shown at 10 bar (green, crossed). (b) Comparison of adsorption (full symbols), diffusion (empty symbols) and membrane (crossed symbols) selectivities computed at infinite dilution and mixture conditions at 1 bar (circles) and 10 bar (stars).

the slow diffusing molecules (CO_2) and slow diffusing molecules can hinder the transport of other gas species. In order to better illustrate the mixture adsorption and diffusion effects, we compared all three selectivities computed at infinite dilution with the ones computed at mixture conditions in Figure 4b. Almost for all the MOFs, S_{ads} is higher at infinite dilution than the mixture case since there is no competitive adsorption at infinite dilution. The diffusivity of CO_2 increases due to the presence of fast CH_4 molecules and diffusivity of CH_4 decreases because of the presence of slow diffusing CO_2 molecules. As a result, S_{diff} values in mixture are higher than those in the infinite dilution as shown in Figure 4b. For example, one of the best performing MOF membranes is SAJFEO at infinite dilution with $P^0_{CO_2}$ of 2×10^8 Barrer and S^0_{mem} of 535. At mixture conditions, permeability and selectivity of this MOF membrane were computed as 3.4×10^5 Barrer and 128, respectively. These dramatic decreases in the membrane properties can be explained by the significant decrease in the adsorption selectivity and increase in the diffusion selectivity. Adsorption selectivity decreased from 12266 at the infinite dilution to 210 whereas diffusion selectivity increased from 0.04 at infinite dilution to 0.61 at

DOI: 10.1021/acssuschemeng.8b05832
ACS Sustainable Chem. Eng. 2019, 7, 2739–2750

Table 1. Performances of the Top 8 MOF Membranes for Separation of Equimolar CO_2/CH_4 Mixture at 1 and 10 bar[a]

MOF	LCD (Å)	PLD (Å)	Volume fraction	N_{CO_2} (mol/kg)	N_{CH_4} (mol/kg)	D_{CO_2} (cm^2/s)	D_{CH_4} (cm^2/s)	P_{CO_2} (Barrer)	P_{CH_4} (Barrer)	S_{ads}	S_{diff}	S_{mem}
						1 bar						
SAJFEO	6.63	6.00	0.60	6.31	0.03	6.16×10^{-6}	1.01×10^{-5}	3.39×10^{5}	2.64×10^{3}	210.33	0.61	128.28
NURVAZ	6.58	6.00	0.60	6.29	0.03	5.52×10^{-6}	1.49×10^{-5}	3.02×10^{5}	3.89×10^{3}	209.67	0.37	77.61
LOYMET	5.37	3.98	0.37	1.43	0.01	1.10×10^{-6}	2.30×10^{-6}	1.47×10^{4}	1.93×10^{2}	158.89	0.48	76.34
KIPKEB	7.31	7.00	0.46	2.65	0.03	3.14×10^{-6}	1.23×10^{-5}	7.74×10^{4}	3.44×10^{3}	88.33	0.25	22.52
KIPJUQ	7.29	6.98	0.46	2.43	0.02	1.78×10^{-6}	1.31×10^{-5}	4.75×10^{4}	2.87×10^{3}	121.50	0.14	16.59
RIPRUF	6.48	4.09	0.59	4.17	0.08	5.86×10^{-6}	3.87×10^{-5}	2.34×10^{5}	2.97×10^{4}	52.13	0.15	7.89
RIPRIT	6.46	4.22	0.60	4.10	0.09	5.73×10^{-6}	4.36×10^{-5}	2.22×10^{5}	3.71×10^{4}	45.56	0.13	5.99
XAXSOG	7.71	5.92	0.63	4.42	0.11	4.65×10^{-6}	4.51×10^{-5}	1.73×10^{5}	4.17×10^{4}	40.18	0.10	4.14
						10 bar						
LOYMET	5.37	3.98	0.37	1.63	0.03	7.21×10^{-7}	2.53×10^{-7}	1.10×10^{3}	7.09×10^{0}	54.33	2.85	154.59
SAJFEO	6.63	6.00	0.60	8.11	0.07	4.02×10^{-6}	3.73×10^{-6}	2.84×10^{4}	2.27×10^{2}	115.86	1.08	125.09
NURVAZ	6.58	6.00	0.60	8.01	0.08	4.10×10^{-6}	3.37×10^{-6}	2.86×10^{4}	2.35×10^{2}	100.13	1.21	121.63
KIPJUQ	7.29	6.98	0.46	3.04	0.03	7.33×10^{-7}	1.71×10^{-6}	2.45×10^{3}	5.63×10^{1}	101.33	0.43	43.45
KIPKEB	7.31	7.00	0.46	3.37	0.04	1.49×10^{-6}	2.89×10^{-6}	4.66×10^{3}	1.08×10^{2}	84.25	0.51	43.35
RIPRIT	6.46	4.22	0.60	6.08	0.28	7.95×10^{-6}	1.31×10^{-5}	4.57×10^{4}	3.47×10^{3}	21.71	0.61	13.17
RIPRUF	6.48	4.09	0.59	6.16	0.22	6.97×10^{-6}	1.95×10^{-5}	4.11×10^{4}	4.11×10^{3}	28.00	0.36	10.00
XAXSOG	7.71	5.92	0.63	7.53	0.32	2.83×10^{-6}	8.62×10^{-6}	1.79×10^{4}	2.32×10^{3}	23.53	0.33	7.73

[a]All selectivities were calculated for CO_2 over CH_4.

Table 2. Comparison of Rigid and Flexible Simulations

	Rigid						Flexible					
MOF	D_{CO_2} (cm^2/s)	D_{CH_4} (cm^2/s)	P_{CO_2} (Barrer)	P_{CH_4} (Barrer)	S_{diff}	S_{mem}	D_{CO_2} (cm^2/s)	D_{CH_4} (cm^2/s)	P_{CO_2} (Barrer)	P_{CH_4} (Barrer)	S_{diff}	S_{mem}
LOYMET	7.21×10^{-7}	2.53×10^{-7}	1096	7	2.85	154.59	1.91×10^{-8}	3.27×10^{-8}	29	0.9	0.58	31.74
KIPJUQ	7.33×10^{-7}	1.71×10^{-6}	2448	56	0.43	43.45	1.43×10^{-7}	6.50×10^{-7}	478	21	0.22	22.34

1 bar. The increase in diffusion selectivity could not compensate the decrease in adsorption selectivity. As a result, predicted separation performance of the membrane (permeability and selectivity) was lower at the mixture case compared to the infinite dilution case. Here, the important point is that mixture permeabilities and selectivities of the top 8 MOF membranes were still high enough to locate them above the Robeson's upper bound as shown in Figure 4a. We also note that in this figure there are two additional upper bounds named as mixture upper bounds which have been established for separation of CO_2/CH_4 mixtures having different compositions.[75] Permeabilities and selectivities obtained from the mixture calculations showed that top MOF membranes exceed the mixture upper bounds. These results suggest that initial screening of MOF membranes based on the membrane properties computed at infinite dilution is efficient to quickly identify the most promising materials and more detailed and computationally expensive mixture simulations should be performed for the top membrane candidates to unlock their actual separation performances at practical operation conditions.

Details on the separation performance of the top 8 MOF membranes at two different feed pressures, 1 and 10 bar, are given in Table 1. As the pressure increases, gas uptakes increase but this increase is more pronounced for CH_4 leading to a decrease in the adsorption selectivities. For most MOFs, diffusivity of both gas molecules decrease with increased pressure as higher loadings hinder the gas diffusion. CH_4 diffusivity is more affected than CO_2 diffusivity because spherical CH_4 molecules are larger and bulkier in size than the linear CO_2 molecules. As a result, higher S_{diff} values were calculated at 10 bar compared to 1 bar for all MOFs. The increase in S_{diff} dominated the decrease in S_{ads} therefore, higher S_{mem} values were observed at 10 bar compared to 1 bar.

All simulations that we discussed so far were carried out using rigid framework assumption. It is known that some MOFs may show inherent flexibility upon various stimuli including pressure, temperature or loading. This flexibility might affect the pore properties of MOFs and change their separation performances.[76] We previously examined the effect of flexibility on the CO_2/CH_4 separation performance of bio-MOFs and showed that flexibility has a significant impact on the permeability and selectivity of MOFs having narrow pore diameters close to the size of adsorbates.[60] Therefore, we carried out computationally demanding flexible MD simulations in the third-level of our calculations for 2 top MOFs, one representing a narrow-pored material (LOYMET) and another representing a large-pored MOF (KIPJUQ). We note that these simulations required significant computation time and resources therefore, we were able to perform them only for 2 representative MOFs. Since the selected 2 MOFs do not have significantly different structural features than the other top materials, similar results are expected for the remaining top MOFs. Results of flexible MD simulations were compared with the results of rigid simulations in Table 2. Gas diffusivities computed using flexible simulations were less than the ones obtained from rigid simulations. Therefore, both permeabilities and selectivities of MOFs were predicted to be lower in flexible case compared to the rigid case as shown in Figure 4a. The decreases in gas permeabilities and selectivities were more pronounced for LOYMET than KIPJUQ since PLD of the former is narrower. For example, membrane selectivity of

DOI: 10.1021/acssuschemeng.8b05832
ACS Sustainable Chem. Eng. 2019, 7, 2739−2750

LOYMET decreased from 155 to 32 while selectivity of KIPJUQ decreased from 43 to 22 when the flexibility was considered. The changes in pore sizes of MOFs were examined using the snapshots taken at different time points of flexible MD simulations by considering the frameworks with and without the adsorbate molecules. As shown in Figure S2a, pore sizes of LOYMET significantly decreased and its PLD became smaller than the kinetic diameter of CH_4 molecule. As a result, diffusivities of both gas molecules were computed to be very slow, in the orders of $\sim 10^8$ cm^2/s. On the other hand, pore sizes of KIPJUQ in the flexible case were still larger than the kinetic diameters of both gases, even when the pores were filled with the adsorbates, resulting in higher CO_2 and CH_4 diffusivities compared to the ones observed in LOYMET. Although gas permeabilities and selectivities of flexible MOFs were found to be lower than the ones computed for rigid MOFs, MOF membranes were still located over the mixed gas upper bound. In other words, the overall assessment about the separation performance of the top MOF membranes did not change even if the structures were flexible.

We so far compared separation performance of MOF membranes with polymers and zeolites and concluded that MOFs can outperform traditional membranes for CO_2/CH_4 separations due to their high gas permeabilities. It is also useful to compare our results with other simulation studies where MOFs are examined. Large numbers of hypothetical MOFs, which are not experimentally synthesized but computer-generated materials, were screened for membrane-based separation of ternary $CO_2/N_2/CH_4$:10/70/20 mixtures using molecular simulations.[35] The best 5 MOFs were computed to have CO_2 permeabilities and CO_2/CH_4 selectivities in the range of 1500−6780 Barrer and 460−8970, respectively at 10 bar, 298 K. We predicted CO_2 permeabilities and CO_2/CH_4 selectivities of MOFs in the range of 1090−45700 Barrer and 7.7−155, respectively for separation of equimolar CO_2/CH_4 mixture at the same pressure and temperature. The lower gas permeabilities and higher membrane selectivities of hypothetical MOFs compared to the real MOFs we considered in this work are due to the narrow pore sizes of the hypothetical MOFs. Hypothetical MOFs were selected to have PLDs between 3 and 4 Å. Since the kinetic diameter of CH_4 is close to 4 Å, hypothetical MOFs act as molecular sieves resulting in high CO_2/CH_4 selectivities. In this work, we especially focused on MOFs having PLDs > 3.75 Å to guarantee the adsorption and diffusion of both CO_2 and CH_4 molecules in the pores. In another study focusing on separation of a ternary mixture of $CO_2/N_2/CH_4$, dominated by N_2 in contrast to our equimolar CO_2/CH_4 binary mixture, the top 7 MOFs were identified using molecular simulations at 10 bar, 298 K.[36] The top MOFs were again selected to have narrow pores in the range of 2.9 < PLD < 3.26 Å and they were computed to have lower permeabilities ($1170 < P_{CO_2} < 5090$ Barrer, $0.18 < P_{CH_4} < 2.61$ Barrer) and higher selectivities ($704 < S_{mem} < 8155$) compared to the ones we calculated for separation of equimolar CO_2/CH_4 mixtures.

We also investigated the impacts of structural belongings on the separation performances of MOFs. Figure 5a shows that porosity of MOFs increases as the LCD increases as expected. We marked the location of the top 8 MOF membranes in Figure 5a. These best membrane candidates have low porosities between 0.4 and 0.6 and narrow pore sizes, LCDs between 5 and 8 Å and PLDs between 4 and 7 Å. Five of the

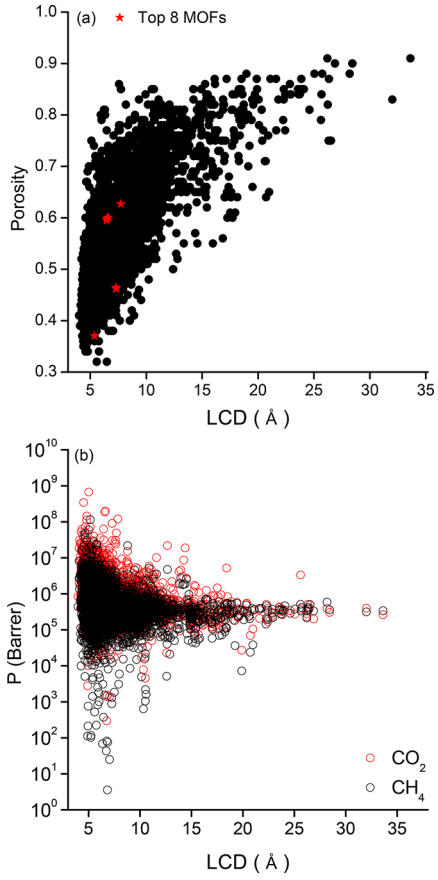


Figure 5. (a) Porosity and LCD of MOFs. Stars represent the top 8 MOF membranes. (b) Gas permeabilities of MOFs as a function of their LCDs.

MOFs overlapped in the figure since they have almost the same porosities, 0.6. Figure 5b shows that permeabilities of CO_2 and CH_4 significantly vary at small LCDs (<10 Å) leading to selective membranes whereas permeabilities of gases become similar as the LCD increases (>10 Å). As shown in Figure 5(a), MOFs with LCDs > 15 Å generally have porosities larger than 0.75 so that both gas molecules can easily adsorb and diffuse in the pores. This eliminates the capability of the pores to sieve the larger gas molecule and leads to lower membrane selectivities. As a result, Figure 5 suggests that membrane materials with small porosities and narrow pore sizes are desired for effective separation of CO_2/CH_4.

MOFs have been widely used as fillers in MMMs to improve the CO_2 permeability and CO_2/CH_4 selectivity of polymers.[77] Motivated from this, we examined the impact of using the top MOFs as fillers in polymer membranes on the CO_2 permeability and CO_2/CH_4 selectivity of MOF-based MMMs. We collected available experimental CO_2/CH_4 mixture permeation data for 8 different polymeric membranes as given in Table S2. This data was then combined with the gas permeability data of the top 8 MOFs obtained from our molecular simulations using Eq. 1. As a result, permeability and selectivity of 64 different MOF-based MMMs were predicted and shown in Figure 6 together with the data of polymer membranes. The arrows represent how the performance (permeability and selectivity) of the polymer membrane changes when the MOF filler is incorporated. Gas permeabilities of the 8 top MOFs are very high compared to the corresponding permeabilities of polymers, cellulose acetate,

DOI: 10.1021/acssuschemeng.8b05832
ACS Sustainable Chem. Eng. 2019, 7, 2739−2750

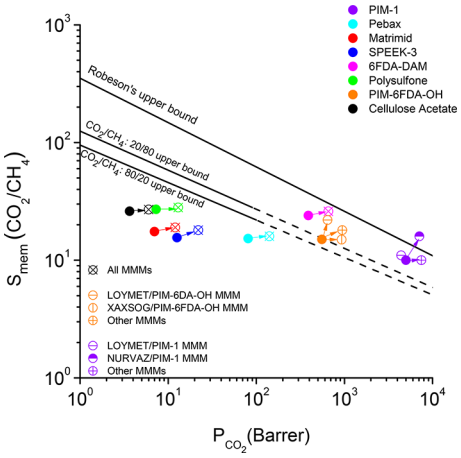


Figure 6. Predicted separation performances of MOF-based MMMs (open symbols) together with separation performances of polymeric membranes (closed symbols).

Matrimid, polysulfone, Pebax, SPEEK-3, and 6-FDA-DAM. For example, P_{CO_2} (P_{CH_4}) of Matrimid is 7 (0.4) Barrer while the lowest P_{CO_2} (P_{CH_4}) among the top 8 MOFs is 1095 (7) Barrer. As shown in previous works,[72,78] when the permeability of filler is very high compared to that of polymer, achievable permeability of the MMM becomes limited. This is because Eq. 1 reduces to $P_{MMM} = P_P \times 1.75$ at a volume fraction of 0.2 if $P_{MOF} \gg P_p$. Therefore, regardless of the identity of the MOF used in a given polymer, similar gas permeabilities and selectivities were obtained for the MMMs and a single data point was used in Figure 6 to represent the MMMs of each polymer except PIM-1 and PIM-6FDA-OH. Incorporation of MOFs into polymers either provides a permeability improvement without significantly affecting the selectivity as in the cases of cellulose acetate, Matrimid, SPEEK-3, Pebax, 6-FDA-DAM and polysulfone or causes a change in both permeability and selectivity as in the cases of PIM-1 and PIM-6FDA-OH. For example, P_{CO_2} of Matrimid increased from 7 to 12 Barrer but its selectivity remained around 18 when MOFs are used as fillers. Since CO_2 and CH_4 permeabilities of MOFs are very high compared to the permeabilities of Matrimid, addition of MOFs increases gas permeabilities without changing the selectivity. For PIM-6FDA-OH, while 6 MOFs caused an increase both in permeability and selectivity, LOYMET significantly increased selectivity with a slight increase in permeability and XAXSOG increased only the permeability. Similarly, for PIM-1, NURVAZ and SAJFEO increased permeability and selectivity. When LOYMET was used as the filler, selectivity of PIM-1 increased at the expense of a reduction in permeability due to the lower CO_2 permeability of LOYMET than that of PIM-1. Other 5 MOFs increased the polymer's permeability without a significant change in selectivity. It is important to highlight the importance of MOF/polymer matching for the separation performance of MOF-based MMMs: While LOYMET provided the highest increase both in permeability and selectivity of PIM-6FDA-OH, the same MOF decreased the permeability of PIM-1. Overall, Figure 6 shows that MOFs can even carry the polymer over the upper bound by increasing both the CO_2 permeability and selectivity if the polymer is close to the upper bound. For example, PIM-6FDA-OH is located just below the upper bound and using LOYMET as a filler significantly improved its CO_2 selectivity from 15 to 22 while increasing its CO_2 permeability from 557 to 960 Barrer. These results suggest that the top MOFs we identified in this work are not only good membrane candidates, but they are also highly promising for making MOF-based MMMs. We would like to note that performances of MOF membranes and MOF/polymer membranes were evaluated based on the Robeson's upper bound. It is important to note that this bound has not been updated since 2008. Several polymer membranes have been developed in the past decade and it is possible that the new polymer membranes may shift the upper bound.

We finally would like to discuss the assumptions used throughout our computational analysis. All our molecular simulations were performed on defect free, perfect, single-crystals of MOFs. In practical applications, MOF membranes may have defects which may significantly affect their separation performances. Therefore, gas permeabilities and selectivities we predicted in this work should be considered as the most optimistic performances that can be expected from an ideal MOF membrane. We only focused on the separation of binary CO_2/CH_4 mixture; however, natural gas may include H_2S and water vapor as impurities that need to be removed. Our molecular simulations cannot provide information about the MOF membranes' stabilities under the presence of these impurities. A recent study showed some MOFs may decompose after H_2S exposure[11] whereas another one reported that some ZIFs degrade in the presence of humid CO_2.[79] Molecular simulation studies also showed that the presence of H_2O may decrease CO_2 adsorption and selectivity of MOFs due to the competitive adsorption between H_2O and CO_2.[80] Similarly, compatibility and stability may be a problem for the MMMs based on the selected MOF−polymer combination. Our MMM calculations did not account for the interactions between the polymer and MOF particles, size distribution and orientation of the MOF fillers in the polymer matrices and simply predicted the separation performances of ideal MOF-based MMMs. However, particle size of the MOF fillers may lead to different concentrations of the nonselective pathways due to the interaction with the polymer and this may have an important effect on the overall separation performance of the MMM. The main motivation of our calculations was to screen very high number of materials to identify a small number of promising MOFs and the issues discussed above can be examined for the top membrane candidates by further experimental efforts.

CONCLUSION

In this work, we combined GCMC and MD simulations to screen 3794 MOF membranes for CO_2/CH_4 separation. In the first-level of screening, we computed gas permeabilities and selectivities of MOFs at infinite dilution to efficiently identify the promising materials. The top 8 MOFs that have CO_2 permeabilities greater than 10^6 Barrer and CO_2/CH_4 selectivities higher than 80 were identified as the best candidates and further studied at the second-level of calculations by performing mixture simulations at two different pressures. Results showed that separation performances of MOF membranes computed at infinite dilution are over-estimated compared to the ones computed at practical operating conditions considering binary gas mixtures. We also showed that the top MOF membrane candidates identified using the simulations at infinite dilution are still located above the upper bound based on their gas permeabilities and

DOI: 10.1021/acssuschemeng.8b05832
ACS Sustainable Chem. Eng. 2019, 7, 2739−2750

selectivities computed using the mixture simulations, indicating the efficiency and validity of our screening approach. We finally performed computationally demanding flexible MD simulations for the two MOFs and showed that these materials are still above the mixed gas upper bound and promising membrane candidates although lower permeabilities and selectivities were estimated compared to the rigid simulations. Materials having narrow pore sizes and low porosities were found to be potential candidates for membrane-based separation of CO_2/CH_4 mixtures. We finally investigated permeabilities and selectivities of 64 different types of MMMs composed of 8 polymers and 8 MOF fillers and showed that incorporation of MOFs significantly enhances CO_2 permeabilities of all polymers and even enhances CO_2/CH_4 selectivities of some polymers. All these results suggest that MOFs can be used as membranes and MMMs for efficient separation of CO_2/CH_4 mixtures. Results of molecular simulations showed that using highly permeable MOFs as pure membranes may be more effective than using them as fillers in polymers since permeability of the MMM is limited when the permeability of filler is very high compared to polymer. The computational screening approach that we used in this work would advance the design and development of MOF membranes and MOF/polymer MMMs by identifying the best MOF candidates and contribute to the sustainable chemistry and engineering in the field of natural gas purification.

■ ASSOCIATED CONTENT

Supporting Information

The Supporting Information is available free of charge on the ACS Publications website at DOI: 10.1021/acssuschemeng.8b05832.

Potentials used in molecular simulations; experimental data for gas separation performances of polymeric membranes; effects of K^0 and D^0 on P^0 of CO_2 and CH_4; change in pore sizes of MOFs (LCD, PLD) in flexible simulations (PDF)

■ AUTHOR INFORMATION

Corresponding Author

*S. Keskin. Email: skeskin@ku.edu.tr. Phone: +90 (212) 338-1362.

ORCID

Seda Keskin: 0000-0001-5968-0336

Notes

The authors declare no competing financial interest.

■ ACKNOWLEDGMENTS

S.K. acknowledges ERC-2017-Starting Grant. This research has received funding from the European Research Council (ERC) under the European Union's Horizon 2020 research and innovation programme (ERC-2017-Starting Grant, grant agreement No 756489-COSMOS).

■ REFERENCES

(1) Guo, A.; Ban, Y. J.; Yang, K.; Yang, W. S. Metal-organic framework-based mixed matrix membranes: Synergetic effect of adsorption and diffusion for CO_2/CH_4 separation. *J. Membr. Sci.* **2018**, *562*, 76−84.

(2) Zhang, Y.; Sunarso, J.; Liu, S. M.; Wang, R. Current status and development of membranes for CO_2/CH_4 separation: A review. *Int. J. Greenhouse Gas Control* **2013**, *12*, 84−107.

(3) Venna, S. R.; Carreon, M. A. Metal organic framework membranes for carbon dioxide separation. *Chem. Eng. Sci.* **2015**, *124*, 3−19.

(4) Li, S.; Falconer, J. L.; Noble, R. D. Improved SAPO-34 membranes for CO_2/CH_4 separations. *Adv. Mater.* **2006**, *18*, 2601−2603.

(5) Falconer, J. L.; Carreon, M. A.; Li, S.; Noble, R. D. Synthesis of zeolites and zeolite membranes using multiple structure directing agents. U.S. Patent 8,302,782, 2012.

(6) Poshusta, J. C.; Tuan, V. A.; Pape, E. A.; Noble, R. D.; Falconer, J. L. Separation of light gas mixtures using SAPO-34 membranes. *AIChE J.* **2000**, *46*, 779−789.

(7) Carreon, M. A.; Li, S.; Falconer, J. L.; Noble, R. D. Alumina-supported SAPO-34 membranes for CO_2/CH_4 separation. *J. Am. Chem. Soc.* **2008**, *130*, 5412−5413.

(8) Li, S.; Zong, Z.; Zhou, S. J.; Huang, Y.; Song, Z.; Feng, X.; Zhou, R.; Meyer, H. S.; Yu, M.; Carreon, M. A. SAPO-34 membranes for N_2/CH_4 separation: Preparation, characterization, separation performance and economic evaluation. *J. Membr. Sci.* **2015**, *487*, 141−151.

(9) Adatoz, E.; Avci, A. K.; Keskin, S. Opportunities and challenges of MOF-based membranes in gas separations. *Sep. Purif. Technol.* **2015**, *152*, 207−237.

(10) Denny, M. S., Jr; Moreton, J. C.; Benz, L.; Cohen, S. M. Metal-organic frameworks for membrane-based separations. *Nat. Rev. Mater.* **2016**, *1*, 1−17.

(11) Liu, J.; Wei, Y. J.; Li, P. Z.; Zhao, Y. L.; Zou, R. Q. Selective H_2S/CO_2 separation by metal-organic frameworks based on chemical-physical adsorption. *J. Phys. Chem. C* **2017**, *121*, 13249−13255.

(12) Trickett, C. A.; Helal, A.; Al-Maythalony, B. A.; Yamani, Z. H.; Cordova, K. E.; Yaghi, O. M. The chemistry of metal-organic frameworks for CO_2 capture, regeneration and conversion. *Nat. Rev. Mater.* **2017**, *2*, 17045.

(13) Zhao, M.; Huang, Y.; Peng, Y.; Huang, Z.; Ma, Q.; Zhang, H. Two-dimensional metal-organic framework nanosheets: synthesis and applications. *Chem. Soc. Rev.* **2018**, *47*, 6267−6295.

(14) Kasik, A.; Lin, Y. S. Organic solvent pervaporation properties of MOF-5 membranes. *Sep. Purif. Technol.* **2014**, *121*, 38−45.

(15) Zhao, Z. X.; Ma, X. L.; Kasik, A.; Li, Z.; Lin, Y. S. Gas separation properties of metal organic framework (MOF-5) membranes. *Ind. Eng. Chem. Res.* **2013**, *52*, 1102−1108.

(16) Zhao, Z. X.; Ma, X. L.; Li, Z.; Lin, Y. S. Synthesis, characterization and gas transport properties of MOF-5 membranes. *J. Membr. Sci.* **2011**, *382*, 82−90.

(17) Yoo, Y.; Lai, Z. P.; Jeong, H. K. Fabrication of MOF-5 membranes using microwave-induced rapid seeding and solvothermal secondary growth. *Microporous Mesoporous Mater.* **2009**, *123*, 100−106.

(18) Liu, Y. Y.; Ng, Z. F.; Khan, E. A.; Jeong, H. K.; Ching, C. B.; Lai, Z. P. Synthesis of continuous MOF-5 membranes on porous alpha-alumina substrates. *Microporous Mesoporous Mater.* **2009**, *118*, 296−301.

(19) Mao, Y. Y.; Cao, W.; Li, J. W.; Liu, Y.; Ying, Y. L.; Sun, L. W.; Peng, X. S. Enhanced gas separation through well-intergrown MOF membranes: seed morphology and crystal growth effects. *J. Mater. Chem. A* **2013**, *1*, 11711−11716.

(20) Nan, J. P.; Dong, X. L.; Wang, W. J.; Jin, W. Q.; Xu, N. P. Step-by-step seeding procedure for preparing HKUST-1 membrane on porous alpha-alumina support. *Langmuir* **2011**, *27*, 4309−4312.

(21) Guerrero, V. V.; Yoo, Y.; McCarthy, M. C.; Jeong, H. K. HKUST-1 membranes on porous supports using secondary growth. *J. Mater. Chem.* **2010**, *20*, 3938−3943.

(22) Liu, D. F.; Ma, X. L.; Xi, H. X.; Lin, Y. S. Gas transport properties and propylene/propane separation characteristics of ZIF-8 membranes. *J. Membr. Sci.* **2014**, *451*, 85−93.

DOI: 10.1021/acssuschemeng.8b05832
ACS Sustainable Chem. Eng. 2019, 7, 2739−2750

(23) Shah, M.; Kwon, H. T.; Tran, V.; Sachdeva, S.; Jeong, H. K. One step in situ synthesis of supported zeolitic imidazolate framework ZIF-8 membranes: Role of sodium formate. *Microporous Mesoporous Mater.* **2013**, *165*, 63−69.
(24) Pan, Y. C.; Wang, B.; Lai, Z. P. Synthesis of ceramic hollow fiber supported zeolitic imidazolate framework-8 (ZIF-8) membranes with high hydrogen permeability. *J. Membr. Sci.* **2012**, *421*, 292−298.
(25) Venna, S. R.; Carreon, M. A. Highly permeable zeolite imidazolate framework-8 membranes for CO_2/CH_4 separation. *J. Am. Chem. Soc.* **2010**, *132*, 76−78.
(26) Huang, A. S.; Liu, Q.; Wang, N. Y.; Caro, J. Organosilica functionalized zeolitic imidazolate framework ZIF-90 membrane for CO_2/CH_4 separation. *Microporous Mesoporous Mater.* **2014**, *192*, 18−22.
(27) Gong, X.; Wang, Y. J.; Kuang, T. R. ZIF-8-based membranes for carbon dioxide capture and separation. *ACS Sustainable Chem. Eng.* **2017**, *5*, 11204−11214.
(28) Erucar, I.; Keskin, S. High-throughput molecular simulations of MOFs for CO_2 separation: Opportunities and challenges. *Front. Mater.* **2018**, *5*, 1−6.
(29) Wu, D.; Yang, Q. Y.; Zhong, C. L.; Liu, D. H.; Huang, H. L.; Zhang, W. J.; Maurin, G. Revealing the structure-property relationships of metal-organic frameworks for CO_2 capture from flue gas. *Langmuir* **2012**, *28*, 12094−12099.
(30) Haldoupis, E.; Nair, S.; Sholl, D. S. Finding MOFs for highly selective CO_2/N_2 adsorption using materials screening based on efficient assignment of atomic point charges. *J. Am. Chem. Soc.* **2012**, *134*, 4313−4323.
(31) Qiao, Z. W.; Zhang, K.; Jiang, J. W. In silico screening of 4764 computation-ready, experimental metal-organic frameworks for CO_2 separation. *J. Mater. Chem. A* **2016**, *4*, 2105−2114.
(32) Altintas, C.; Erucar, I.; Keskin, S. High-throughput computational screening of the metal organic framework database for CH_4/H_2 separations. *ACS Appl. Mater. Interfaces* **2018**, *10*, 3668−3679.
(33) Watanabe, T.; Sholl, D. S. Accelerating applications of metal-organic frameworks for gas adsorption and separation by computational screening of materials. *Langmuir* **2012**, *28*, 14114−14128.
(34) Daglar, H.; Keskin, S. Computational screening of metal-organic frameworks for membrane-based $CO_2/N_2/H_2O$ separations: Best materials for flue gas separation. *J. Phys. Chem. C* **2018**, *122*, 17347−17357.
(35) Qiao, Z. W.; Peng, C. W.; Zhou, J.; Jiang, J. W. High-throughput computational screening of 137953 metal-organic frameworks for membrane separation of a $CO_2/N_2/CH_4$ mixture. *J. Mater. Chem. A* **2016**, *4*, 15904−15912.
(36) Qiao, Z. W.; Xu, Q. S.; Jiang, J. W. High-throughput computational screening of metal-organic framework membranes for upgrading of natural gas. *J. Membr. Sci.* **2018**, *551*, 47−54.
(37) Altintas, C.; Avci, G.; Daglar, H.; Gulcay, E.; Erucar, I.; Keskin, S. Computer simulations of 4240 MOF membranes for H_2/CH_4 separations: Insights into structure-performance relations. *J. Mater. Chem. A* **2018**, *6*, 5836−5847.
(38) Avci, G.; Velioglu, S.; Keskin, S. High-throughput screening of MOF adsorbents and membranes for H_2 purification and CO_2 capture. *ACS Appl. Mater. Interfaces* **2018**, *10*, 33693−33706.
(39) Haldoupis, E.; Watanabe, T.; Nair, S.; Sholl, D. S. Quantifying large effects of framework flexibility on diffusion in MOFs: CH_4 and CO_2 in ZIF-8. *ChemPhysChem* **2012**, *13*, 3449−3452.
(40) Fairen-Jimenez, D.; Galvelis, R.; Torrisi, A.; Gellan, A. D.; Wharmby, M. T.; Wright, P. A.; Mellot-Draznieks, C.; Duren, T. Flexibility and swing effect on the adsorption of energy-related gases on ZIF-8: combined experimental and simulation study. *Dalton Trans.* **2012**, *41*, 10752−10762.
(41) Moghadam, P. Z.; Li, A.; Wiggin, S. B.; Tao, A.; Maloney, A. G. P.; Wood, P. A.; Ward, S. C.; Fairen-Jimenez, D. Development of a Cambridge Structural Database subset: A collection of metal-organic frameworks for past, present, and future. *Chem. Mater.* **2017**, *29*, 2618−2625.
(42) Willems, T. F.; Rycroft, C. H.; Kazi, M.; Meza, J. C.; Haranczyk, M. Algorithms and tools for high-throughput geometry-based analysis of crystalline porous materials. *Microporous Mesoporous Mater.* **2012**, *149*, 134−141.
(43) Dubbeldam, D.; Calero, S.; Ellis, D. E.; Snurr, R. Q. RASPA: Molecular simulation software for adsorption and diffusion in flexible nanoporous materials. *Mol. Simul.* **2016**, *42*, 81−101.
(44) Frenkel, D.; Smit, B. *Understanding Molecular Simulation: From Algorithms to Applications*, 2nd ed.; Academic Press: San Diego, 2002.
(45) Potoff, J. J.; Siepmann, J. I. Vapor-liquid equilibria of mixtures containing alkanes, carbon dioxide, and nitrogen. *AIChE J.* **2001**, *47*, 1676−1682.
(46) Rappe, A. K.; Casewit, C. J.; Colwell, K. S.; Goddard, W. A.; Skiff, W. M. UFF, a full periodic table force field for molecular mechanics and molecular dynamics simulations. *J. Am. Chem. Soc.* **1992**, *114*, 10024−10035.
(47) Wilmer, C. E.; Snurr, R. Q. Towards rapid computational screening of metal-organic frameworks for carbon dioxide capture: Calculation of framework charges via charge equilibration. *Chem. Eng. J.* **2011**, *171*, 775−781.
(48) Rappe, A. K.; Goddard, W. A., III Charge equilibration for molecular dynamics simulations. *J. Phys. Chem.* **1991**, *95*, 3358−3363.
(49) Ewald, P. P. Die berechnung optischer und elektrostatischer gitterpotentiale. *Ann. Phys.* **1921**, *369*, 253−287.
(50) Sumer, Z.; Keskin, S. Ranking of MOF adsorbents for CO_2 separations: A molecular simulation study. *Ind. Eng. Chem. Res.* **2016**, *55*, 10404−10419.
(51) Ozturk, T. N.; Keskin, S. Computational screening of porous coordination networks for adsorption and membrane-based gas separations. *J. Phys. Chem. C* **2014**, *118*, 13988−13997.
(52) Dzubak, A. L.; Lin, L.-C.; Kim, J.; Swisher, J. A.; Poloni, R.; Maximoff, S. N.; Smit, B.; Gagliardi, L. Ab initio carbon capture in open-site metal-organic frameworks. *Nat. Chem.* **2012**, *4*, 810−816.
(53) Boyd, P. G.; Moosavi, S. M.; Witman, M.; Smit, B. Force-field prediction of materials properties in metal-organic frameworks. *J. Phys. Chem. Lett.* **2017**, *8*, 357−363.
(54) Bristow, J. K.; Tiana, D.; Walsh, A. Transferable force field for metal-organic frameworks from first-principles: BTW-FF. *J. Chem. Theory Comput.* **2014**, *10*, 4644−4652.
(55) Dubbeldam, D.; Torres-Knoop, A.; Walton, K. S. On the inner workings of Monte Carlo codes. *Mol. Simul.* **2013**, *39*, 1253−1292.
(56) Keskin, S.; Sholl, D. S. Assessment of a metal-organic framework membrane for gas separations using atomically detailed calculations: CO_2, CH_4, N_2, H_2 mixtures in MOF-5. *Ind. Eng. Chem. Res.* **2009**, *48*, 914−922.
(57) Adatoz, E.; Keskin, S. Application of MD simulations to predict membrane properties of MOFs. *J. Nanomater.* **2015**, *2015*, 1−9.
(58) Dassault Systèmes BIOVIA. *Materials Studio*, 2017 R2; Dassault Systèmes: San Diego, 2018.
(59) Akkermans, R. L. C.; Spenley, N. A.; Robertson, S. H. Monte Carlo methods in Materials Studio. *Mol. Simul.* **2013**, *39*, 1153−1164.
(60) Erucar, I.; Keskin, S. Computational modeling of bioMOFs for CO_2/CH_4 separations. *Chem. Eng. Sci.* **2015**, *130*, 120−128.
(61) Garberoglio, G.; Taioli, S. Modeling flexibility in metal-organic frameworks: Comparison between density-functional tight-binding and universal force field approaches for bonded interactions. *Microporous Mesoporous Mater.* **2012**, *163*, 215−220.
(62) Houde, A.; Krishnakumar, B.; Charati, S.; Stern, S. Permeability of dense (homogeneous) cellulose acetate membranes to methane, carbon dioxide, and their mixtures at elevated pressures. *J. Appl. Polym. Sci.* **1996**, *62*, 2181−2192.
(63) Khan, A. L.; Li, X.; Vankelecom, I. F. SPEEK/Matrimid blend membranes for CO_2 separation. *J. Membr. Sci.* **2011**, *380*, 55−62.
(64) Guo, X.; Huang, H.; Ban, Y.; Yang, Q.; Xiao, Y.; Li, Y.; Yang, W.; Zhong, C. Mixed matrix membranes incorporated with amine-functionalized titanium-based metal-organic framework for CO_2/CH_4 separation. *J. Membr. Sci.* **2015**, *478*, 130−139.

DOI: 10.1021/acssuschemeng.8b05832
ACS Sustainable Chem. Eng. 2019, 7, 2739−2750

(65) Khan, A. L.; Li, X.; Vankelecom, I. F. Mixed-gas CO_2/CH_4 and CO_2/N_2 separation with sulfonated PEEK membranes. *J. Membr. Sci.* **2011**, *372*, 87−96.
(66) Khosravi, T.; Omidkhah, M.; Kaliaguine, S.; Rodrigue, D. Amine-functionalized CuBTC/poly (ether-b-amide-6)(Pebax® MH 1657) mixed matrix membranes for CO_2/CH_4 separation. *Can. J. Chem. Eng.* **2017**, *95*, 2024−2033.
(67) Bae, T. H.; Lee, J. S.; Qiu, W.; Koros, W. J.; Jones, C. W.; Nair, S. A high-performance gas-separation membrane containing submicrometer-sized metal-organic framework crystals. *Angew. Chem.* **2010**, *122*, 10059−10062.
(68) Swaidan, R.; Ghanem, B. S.; Litwiller, E.; Pinnau, I. Pure-and mixed-gas CO_2/CH_4 separation properties of PIM-1 and an amidoxime-functionalized PIM-1. *J. Membr. Sci.* **2014**, *457*, 95−102.
(69) Swaidan, R.; Ma, X.; Litwiller, E.; Pinnau, I. High pressure pure-and mixed-gas separation of CO_2/CH_4 by thermally-rearranged and carbon molecular sieve membranes derived from a polyimide of intrinsic microporosity. *J. Membr. Sci.* **2013**, *447*, 387−394.
(70) Erucar, I.; Keskin, S. Screening metal-organic framework-based mixed - matrix membranes for CO_2/CH_4 separations. *Ind. Eng. Chem. Res.* **2011**, *50*, 12606−12616.
(71) Maxwell, J. C. *A Treatise on Electricity and Magnetism*; Dover Publications, 1954.
(72) Bouma, R.; Checchetti, A.; Chidichimo, G.; Drioli, E. Permeation through a heterogeneous membrane: The effect of the dispersed phase. *J. Membr. Sci.* **1997**, *128*, 141−149.
(73) Kim, J.; Abouelnasr, M.; Lin, L.-C.; Smit, B. Large-scale screening of zeolite structures for CO_2 membrane separations. *J. Am. Chem. Soc.* **2013**, *135*, 7545−7552.
(74) Robeson, L. M. The upper bound revisited. *J. Membr. Sci.* **2008**, *320*, 390−400.
(75) Lin, H.; Yavari, M. Upper bound of polymeric membranes for mixed-gas CO_2/CH_4 separations. *J. Membr. Sci.* **2015**, *475*, 101−109.
(76) Caro, J. Are MOF membranes better in gas separation than those made of zeolites? *Curr. Opin. Chem. Eng.* **2011**, *1*, 77−83.
(77) Dechnik, J.; Gascon, J.; Doonan, C. J.; Janiak, C.; Sumby, C. J. Mixed-matrix membranes. *Angew. Chem., Int. Ed.* **2017**, *56*, 9292−9310.
(78) Yilmaz, G.; Keskin, S. Molecular modeling of MOF and ZIF-filled MMMs for CO_2/N_2 separations. *J. Membr. Sci.* **2014**, *454*, 407−417.
(79) Bhattacharyya, S.; Jayachandrababu, K. C.; Chiang, Y. D.; Sholl, D. S.; Nair, S. Butanol separation from humid CO_2-containing multicomponent vapor mixtures by zeolitic imidazolate frameworks. *ACS Sustainable Chem. Eng.* **2017**, *5*, 9467−9476.
(80) Yu, J. M.; Wu, Y. F.; Balbuena, P. B. Response of metal sites toward water effects on postcombustion CO_2 capture in metal-organic frameworks. *ACS Sustainable Chem. Eng.* **2016**, *4*, 2387−2394.

DOI: 10.1021/acssuschemeng.8b05832
ACS Sustainable Chem. Eng. 2019, 7, 2739−2750